Mem. S.A.It. Vol. 77, 916

Memorie della

A new approach to the ^{176}Lu puzzle

F. Käppeler[1], N. Winckler[1], S. Dababneh[1,2], M. Heil[1], S. Bisterzo[3], and R. Gallino[3,4]

[1] Institut für Kernphysik, Forschungszentrum Karlsruhe, 76021 Karlsruhe, Germany
[2] Institute for Science and Information Technology, AlBalqa Applied University, Salt, Jordan
[3] Dipartimento di Fisica Generale, Università di Torino, Sezione INFN di Torino, Via P. Giuria 1, I-10125 Torino, Italy
[4] Centre for Stellar and Planetary Astrophysics, School of Mathematical Sciences, Monash University, PO Box 28M, Victoria 3800, Australia e-mail: franz.kaeppeler@ik.fzk.de

Abstract. The *s*-process branching at A = 176 has been analyzed on the basis of significantly improved experimental results for the partial and total (n,γ) cross sections of the involved Lu and Hf isotopes. The measurements, which were carried out at the Karlsruhe 3.7 MV Van de Graaff accelerator, are summarized and the results are compared with previous data. On the basis of this improved nuclear physics input, a comprehensive analysis of the branching at ^{176}Lu was carried out for testing the temperature conditions during He shell flashes in thermally pulsing low mass asymptotic giant branch stars.

1. Introduction

Lutetium is the last rare earth element (REE) and is followed in atomic number by the element hafnium. Due to its long half-life of 36 Gy, ^{176}Lu was initially considered as a potential nuclear chronometer for the age of the *s* elements. This possibility is based on the fact that ^{176}Lu as well as its daughter ^{176}Hf are of pure *s*-process origin, since both are shielded against the *r*-process beta decay chains by their stable isobar ^{176}Yb (Fig. 1). However, it was found that the thermal photon bath at typical *s*-process temperatures is energetic enough for induced transitions from the long-lived ground state to the short-lived isomer ($t_{1/2}$ = 3.68 h), thus dramatically reducing the effective half-life to a few hours. This effect changes the information contained in the ^{176}Lu/^{176}Hf pair from a potential chronometer into a sensitive *s*-process thermometer (Beer et al. 1981; Klay et al. 1991; Doll et al. 1999).

As far as the stellar neutron capture rates are concerned, very accurate total (n,γ) cross sections have recently been obtained for ^{175}Lu and ^{176}Lu in a time-of-flight (TOF) measurement using a 4π BaF_2 array (Wisshak et al. 2006a). The Maxwellian averaged cross sections (MACS) deduced from these data are five times more accurate than the values listed in the compilation of Bao *et al.* (2000). In case of ^{175}Lu it has to be considered that neutron captures may feed either the ground state or the isomer in ^{176}Lu. Therefore, the total (n,γ) cross section has to be complemented by a measurement of at least one of the two partial cross sections. Since the corresponding reaction channels could not be distinguished in the TOF measurement, the activation technique

Send offprint requests to: F. Käppeler

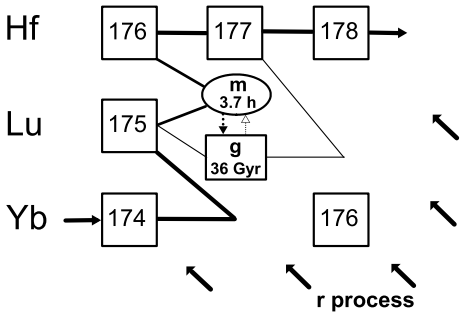

Fig. 1. The *s*-process reaction flow in the Lu region. The strength of the lines indicates that neutron captures leading to the isomeric state are more probable than to the ground state. See text for the connecting arrows between ^{176}Lu^{g} and ^{176}Lu^{m}.

has been employed to determine the partial cross section to the isomeric state ^{176}Lu^{m} at thermal energies of kT = 5 and 25 keV. The measurements and data analysis are described in Secs. 2 and 3, followed by a discussion of the astrophysical implications in Sec. 4.

2. Measurements

The activation measurements on ^{175}Lu were carried out at the Karlsruhe 3.7 MV pulsed Van de Graaff accelerator using two reactions for producing quasi-stellar neutron spectra close to the characteristic temperatures of the relevant neutron source reactions of the *s* process. Near the typical thermal energy of the ^{13}C$(\alpha, n)^{16}$O reaction at kT = 8 keV, a neutron spectrum corresponding to kT = 5.1 ± 0.1 keV was obtained via the ^{18}O$(p, n)^{18}$F reaction by choosing the proton energy 8 keV above the reaction threshold of E_p = 2574 keV (Heil et al. 2005). This reaction, though hampered by a comparably low (p, n) cross section, is an important complement to the more prolific ^{7}Li$(p, n)^{7}$Be reaction. The neutron spectrum that can be produced via the ^{7}Li$(p, n)^{7}$Be reaction represents the experimental counterpart of the second most important stellar neutron source provided by the ^{22}Ne$(\alpha, n)^{25}$Mg reaction. In this case the spectrum mimics a thermal energy of kT = 25 keV, also rather close to the 23 keV typical of the He shell flashes in low mass AGB stars (see also Heil et al., this volume).

The Lu samples were cut from 0.1 mm and 0.2 mm thick foils of natural composition. During the irradiations, each foil was sandwiched between two 0.03 mm thick gold foils of the same diameter since all activation measurements are normalized to gold. In spite of the large self absorption correction for the 88 keV γ-ray line in the decay of ^{176}Lu^{m}, the choice of the rather thick samples was dictated by the low neutron intensity of the ^{18}O$(p, n)^{18}$F reaction. Correspondingly, special attention was paid to the reliable determination of this effect.

The ^{18}O targets were deposited on 0.2 mm thick tantalum disks by electrolysis of water enriched to 95% in ^{18}O. In total, four targets with an oxide layer about 2 μm in thickness were produced. These targets were glued onto a copper backing 1 mm in thickness, which is cooled by lateral heat conduction to a water cooled copper ring. Since the proton energy is adjusted slightly above the reaction threshold, all neutrons are emitted in a forward cone of 140 deg opening angle. Thus, moderation effects are avoided by the ring geometry. Effects due to neutron scattering in the copper backing are negligible because of the 98% transmission for neutrons in the energy range of interest.

The ^{7}Li targets consisted of metallic layers of natural lithium, which were directly evaporated onto the copper backings. The layers were 30 μm in thickness.

During the irradiations, the time history of the neutron flux was registered by means of a ^{6}Li glass detector, which was placed on the proton beam axis at a distance of 1 m from the target. This information is relevant in order to determine the factor f_b for the proper correction for the fraction of nuclei, which decayed already during irradiation (Sec.3.1). The proton beam of typically 40 μA was wobbled across the lithium target to ensure homogeneous illumination. The irradiations were carried out by placing the samples in direct contact with the neutron target as described elsewhere (Ratzel et al. 2004).

After irradiation, the induced activity was measured with a γ-detection system consisting

of two high purity germanium clover detectors. Each clover detector consists of four independent HPGe n-type crystals in a common cryostat. Each crystal is 50 mm in diameter and about 70 mm in length. The front part of the crystals in one of the two clovers is tapered. The total crystal volume of the detector system is about 1000 cm^3.

The two clover detectors were placed face to face in close proximity such that they were in contact with the 5.2 mm thick sample holder. This holder is designed to guarantee an exact and reproducible positioning of the sample in the very center of the system. The whole assembly, which forms nearly a 4π geometry, was covered with 10 cm of lead in order to decrease the room background. The number of net counts in the relevant γ-lines are determined by a fit of the line and the surrounding background.

The analysis was based on the most intense line in the decay of the isomeric state with E_γ = 88.36 keV. The decay properties of all relevant states, which were used in the analysis, were adopted from Chunmei (1995) and Browne and Junde (1998).

3. Analysis and results

At the end of each irradiation, the number of activated nuclei in the sample and in the gold foils are

$$A = \phi_T \;\; N \;\; \sigma \;\; f_b. \tag{1}$$

In this expression ϕ_T is the time integrated neutron flux, N the number of sample atoms per cm^2, σ the capture cross section, and f_b a correction factor that accounts for the decay and for the variation of the neutron flux during the irradiation.

Since all measurements are performed relative to ^{197}Au, Eq. (1) yields

$$\frac{A_i}{A_{\rm Au}} = \frac{\sigma_i \;\; N_i \;\; f_{b_i}}{\sigma_{\rm Au} N_{\rm Au} f_{b_{\rm Au}}} \tag{2}$$

where A_i and $A_{\rm Au}$ are determined by the respective net counts registered in the detector.

The decay of the isomeric state has to be distinguished from the decay of the ground state, which - in spite of its long half-life - is producing the 88 keV transition in ^{176}Hf at a comparable level. Therefore, the activity of the irradiated Lu samples was first measured after a short waiting time t_{w_1} in order to determine the total counts $C_{tot} = C_g + C_m$, including the decay of the isomer plus the decay of the ^{176}Lu$^{\rm g}$ contained in the natural sample. After an additional waiting time $t_{w_2} \gg t_{1/2}(^{176}{\rm Lu}^{\rm m})$, all ^{176}Lu$^{\rm m}$ had decayed and the correction for the ground state contribution could be obtained. This contribution is then subtracted from the first measurement.

Because of the low γ-energy emitted in the decay of ^{176}Lu$^{\rm m}$, considerable effort was devoted to the accurate determination of the corresponding self-absorption correction. For a distant point source the correction for self absorption can be obtained as $K_\gamma = \frac{1-e^{-\mu d}}{\mu d}$, where μ the self absorption coefficient and d is the sample thickness (Beer and Käppeler 1980). The close geometry of the present experiment, which was necessary because of the weak activities produced in the 5 keV irradiations, required, however, that K_γ were evaluated by comprehensive GEANT4 simulations. In these simulations minor effects due to the extended sample size and cascade summing have been included as well.

Since the experimental MACS of gold at kT = 5.1 keV is not yet available, the reference cross section has been evaluated from the ENDF/B data base, which was normalized to the experimental MACS at kT = 30 keV. The adopted MACS of gold at kT = 5.1 keV is (Heil et al. 2005)

$$\frac{\langle \sigma {\rm v} \rangle}{{\rm v}_T} = 2028 \pm 50 \text{ mb}.$$

The weighted MACS for the partial (n,γ) cross section to the isomeric state of ^{176}Lu is

$$\frac{\langle \sigma(^{175}{\rm Lu}^{\rm m}){\rm v} \rangle}{{\rm v}_T} = 3048 \pm 195 \text{ mb}.$$

The uncertainty of the present measurement is clearly dominated by systematic effects, particularly by the intensity of the 88 keV line in the decay of ^{176}Lu$^{\rm m}$ and by the efficiency of the HPGe detectors.

In principle, the 5% uncertainty introduced by the relative intensity of the 88 keV γ-transition could be reduced by a more accurate measurement of the decay scheme. In the present analysis, the problem with this uncertainty was circumvented by comparison with the previous activations of Zhao and Käppeler (1991) at kT = 25 keV, where partial cross sections of 1153 ± 25 mb and 1101 ± 24 mb have been obtained by spectroscopy of the electrons emitted in the decay of ^{176}Lu^{m} as well as by detecting the 88 keV γ transition.

The total capture cross section of ^{175}Lu has been accurately measured by Wisshak *et al.* (2006a). These authors report MACS for thermal energies between kT = 8 keV and 100 keV. Combining their value at kT = 25 keV with the normalized partial cross section of 1153 ± 25 mb leads to an isomeric ratio of $IR(kT = 25\ \mathrm{keV}) = 0.857 \pm 0.023$.

At the lower thermal energy of kT = 5 keV the present measurement yields a partial cross section of 3185 ± 97 mbarn. The total capture cross section at kT = 5 keV was determined to be 3568 ± 75 mb following the prescription of Wisshak *et al.* (2006a). With these data, the isomeric ratio becomes $IR(kT = 5\ \mathrm{keV}) = 0.893 \pm 0.037$.

4. The ^{176}Lu branching and the *s*-process temperature

4.1. Nuclear Input

In addition to the experimental cross sections of ^{175}Lu reported here, MACSs of the other involved isotopes and the respective stellar enhancement factors were taken from Bao *et al.* (2000) and from the recent work of Wisshak et al. (2006a, 2006b).

The isomeric ratios in the keV region that are obtained by combining the total (n,γ) cross section data with the present results are significantly larger than at thermal neutron energy. Within uncertainties, the present results at kT = 5 keV and 25 keV are in fair agreement. Therefore, a weighted average of 0.87 ± 0.03 has been adopted for the branching analysis. This result is compatible but more accurate than the value of 0.90 ± 0.04 derived on the basis of earlier cross sections (Bao et al. 2000), and 8% higher than theoretically predicted.

The half-life of ^{176}Lu was shown to decrease drastically at the temperatures reached during stellar He burning (Klay et al. 1991; Doll et al. 1999). Contrary to the situation at low excitation energy, where transitions between ground state and isomer are strictly forbidden by selection rules, interaction with thermal photons induce transitions to higher lying nuclear states, which can decay into the ground state and into the isomer as well. This thermal coupling can, therefore, lead to a destruction of the long-lived ground state.

While thermal effects are negligible below T_8 = 1.5, where T_8 is the temperature in units of 10^8 K, the population probabilities of ground state and isomer start to be increasingly coupled between T_8 = 2.2 and 3.0, resulting in a strong reduction of the effective half-life, but also to an additional feeding of the ground state. It is due to this effect that more ^{176}Lu is observed in nature than would be created in a "cool" environment. In this regime, internal transitions, β-decays, and neutron captures are equally important and have to be properly considered during He shell flashes, where the final abundance pattern of the *s*-process branchings are formed.

The thermal effects sketched above were treated by using the temperature-dependent beta decay rate of ^{176}Lu from the work of Doll et al. (1999), and the branching factor as a function of temperature and neutron density (Fig.2) was determined following the prescription of Klay et al. (1991) complemented by the updated input from Doll et al. (1999). This information is most crucial for the proper treatment of the strong temperature gradient in the bottom layers of the He shell flashes. Accordingly, the convective region of the He shell flashes was subdivided into 20 zones and the ^{176}Lu production and decay was followed over these layers numerically as described below.

The Lu/Hf abundance ratio is required as an additional input for the branching analysis. The adopted value of 0.239 has been taken from the work of Blichert-Toft and Albarède (1997), which is confirmed by data

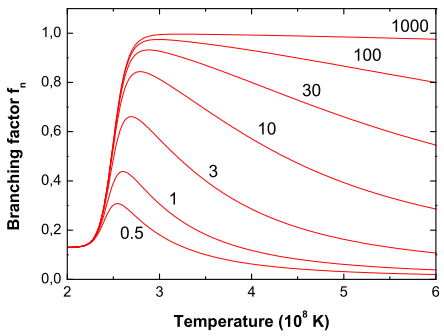

Fig. 2. The branching factor f_n as a function of temperature and neutron density (in units of 10^8 cm^{-3}). The plot covers the transition region between the low temperature regime, characterized by the initial population probabilities due to neutron capture, and the high temperature regime, where complete thermal equilibrium is achieved. Below $T_8 = 2$, the branching factor is defined by the partial cross sections to ground state and isomer, independent of temperature and neutron density.

from Bizzarro et al. (2003) and is in perfect agreement with the value in the widely used solar system abundance table of Anders and Grevesse (1989).

4.2. Stellar Model

Over the last decade, considerable progress in stellar modeling has led to an increasingly quantitative picture of the *s* process, in particular with respect to the main *s*-process component associated with the He intershell of thermally pulsing Asymptotic Giant Branch (AGB) stars (see Busso, Gallino, & Wasserburg 1999). During this AGB phase, neutrons are alternatively released by two sources: the reactions ^{13}C$(\alpha,n)^{16}$O and ^{22}Ne$(\alpha,n)^{25}$Mg. The first reaction operates radiatively in a tiny region of the He intershell (the so-called ^{13}C pocket) at $T = 10^8$ K ($kT = 8$ keV) during the shell hydrogen burning phase and provides more than 90% of the total neutron exposure. The second reaction occurs during the short but intense helium shell flashes at typical temperatures close to $T_8 = 3$ ($kT = 23$ keV).

Although the second neutron burst during the He shell flashes contributes only a few percent to the total neutron exposure, the final composition of the Lu/Hf branching is, in fact, established during the decrease of the neutron density after the thermal pulse. This phase is also essential for the thermal coupling between ground state and isomer, which is effective during this high-temperature phase. In this context, it is important to note that the (n,γ) cross sections in the Lu/Hf region are large enough that typical neutron capture times are significantly shorter than the duration of the neutron exposure during the He shell flash.

The current calculations of AGB nucleosynthesis were based on the standard assumptions, which have been shown to match the solar main *s*-process component fairly well (Arlandini et al. 1999), i.e. using the average of models for 1.5 $M_\odot$ and 3 $M_\odot$, a metallicity of 0.5 $Z_\odot$, and the standard ^{13}C pocket (Gallino et al. 1998).

4.3. Branching Analysis

The abundances obtained in the stellar model calculations were normalized to the reference isotope ^{150}Sm. In the investigated stellar scenario too much of ^{175}Hf and somewhat too little of ^{176}Lu$^{\rm g}$ is produced during the main neutron exposure provided by the ^{13}C$(\alpha,n)^{16}$O reaction, where temperatures are too low for causing a thermal depopulation of the isomer. As indicated in Fig. 2 this additional feeding of the long-lived ground state occurs only at the higher temperatures during He shell flashes, leading to a strong increase in the production of ^{176}Lu$^{\rm g}$.

This behavior is illustrated in Fig. 3 showing the relative production factors of ^{176}Lu and ^{176}Hf. One finds that ^{176}Hf is almost completely destroyed at the beginning of the flash, when neutron density and temperature are highest. Under these conditions, ^{176}Hf is efficiently bypassed by the reaction flow (Fig. 2), resulting in a corresponding production of ^{176}Lu. As temperature and neutron density decline with time, the branching towards ^{176}Hf is more and more restored, but the final abun-

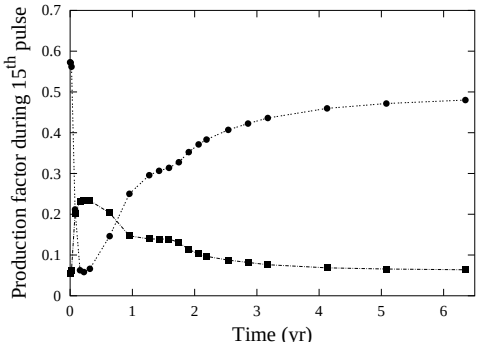

Fig. 3. The production factors of ^{176}Lu (squares) and of ^{176}Hf (circles) during the 15th He shell flash in an AGB star with 1.5 $M_\odot$. The time scale starts when the temperature at the bottom of the convective shell reaches 2.5×10^8 K, i.e. at the onset of the ^{22}Ne(α, n)^{25}Mg reaction. The curves are normalized to ^{150}Sm at the end of the He shell flash.

dance at the end of the He shell flash remains significantly lower than before.

Compared to a similar previous study (Arlandini et al. 1999), the now available, improved cross section information appears to settle the the ^{176}Lu puzzle. While the ^{176}Hf abundance was before overproduced by 10 - 20%, the present calculations yield final ^{176}Lu^{g} and ^{176}Hf abundances (relative to solar system values) of 1.04 and 0.96, respectively. These results do not yet consider the decay of the produced ^{176}Lu^{g} prior to the formation of the solar system, a correction that would bring the two numbers into close agreement. A quantitative estimate of this aspect has to be evaluated in the context of a galactic chemical evolution model.

Acknowledgements. We thank G. Rupp for excellent technical support as well as the accelerator crew E.-P. Knaetsch, D. Roller, and W. Seith for perfect beam conditions. This work was supported by the Italian MIUR-FIRB Project "The astrophysical origin of the heavy elements beyond Fe"

References

Anders, E. & Grevesse, N. 1989, Geochim. Cosmochim. Acta, 53, 197
Arlandini, C., Käppeler, F., Wisshak, K., Gallino, R., Lugaro, M., Busso, M., & Straniero, O. 1999, ApJ, 525, 886
Bao, Z.Y., Beer, H., Käppeler, F., Voss, F., Wisshak, K., & Rauscher, T. 2000, Atomic Data Nucl. Data Tables, 76, 70
Beer, H. & Käppeler, F. 1980, Phys. Rev. C, 21, 534
Beer, H., Käppeler, F., Wisshak, K., & Ward, R.A. 1981, ApJ Suppl., 46, 295
Bizzarro, M., Baker, J. A., Haack, H., Ulfbeck, D., & Rosing, M. 2003, Nature, 421, 931
Blichert-Toft, J. & Albarède, F. 1997, Earth Planet. Sci. Lett., 148, 243
Browne, E. & Junde, H. 1998, Nuclear Data Sheets, 84, 400
Busso, M., Gallino, R., & Wasserburg, G.J. 1999, Annu. Rev. Astron. Astrophys., 37, 239
Chunmei, Z. 1995, Nucl. Data Sheets, 74, 259
Doll, C., Börner, H., Jaag, S., & Käppeler, F. 1999, Phys. Rev. C, 59, 492
Gallino, R., Arlandini, C., Busso, M., Lugaro, M., Travaglio, C., Straniero, O., Chieffi, A., & Limongi, M. 1998, ApJ, 497, 388
Heil, M., Dababneh, S., Juseviciute, A., Käppeler, F., Plag, R., Reifarth, R., & O'Brien, S. 2005, Phys. Rev. C, 71, 025803
Klay, N., Käppeler, F., Beer, H., & Schatz, G. 1991, Phys. Rev. C, 44, 2839
Ratzel, U., Arlandini, C., Käppeler, F., Couture, A., Wiescher, M., Reifarth, R., Gallino, R., Mengoni, A., & Travaglio, C. 2004, Phys. Rev. C, 70, 065803
Wisshak, K., Voss, F., Käppeler, F., & Kazakov, L. 2006a, Phys. Rev. C, 73, 015807
Wisshak, K., Voss, F., Käppeler, F., Kazakov, L., Bečvář, F., Krtička, M., Gallino, R. & Pignatari, M. 2006b, Phys. Rev. C, in press
Zhao, W.R. & Käppeler, F. 1991, Phys. Rev. C, 44, 506